

Crystal Structure and Nonlinear Optical Properties of KSnOPO_4 and their Comparison with KTiOPO_4

BY P. A. THOMAS, A. M. GLAZER AND B. E. WATTS

Clarendon Laboratory, Parks Road, Oxford OX1 3PU, England

(Received 9 November 1989; accepted 22 January 1990)

Abstract

Crystals of KTiOPO_4 (potassium titanyl phosphate, KTP) and its tin analogue KSnOPO_4 (potassium stannyl phosphate, KSP), were grown and characterized for their structural and nonlinear optical properties. The crystal structure of KTiOPO_4 [$M_r = 197.97$, orthorhombic, space group $Pna2_1$ (C_{2v}^9), $a = 12.819$ (3), $b = 6.399$ (1), $c = 10.584$ (2) Å, $V = 868.1$ Å³] was refined to an R factor of 2.5% from room-temperature single-crystal X-ray data. Using the refined coordinates, a model for the centrosymmetric prototype phase with suggested space group $Pnan$ (D_{2h}^6) is constructed. From this model, the magnitude and direction of the spontaneous polarization developed in the room-temperature crystal structure are calculated. The crystal structure of KSnOPO_4 [$M_r = 268.76$, orthorhombic, space group $Pna2_1$, $a = 13.145$ (3), $b = 6.526$ (2), $c = 10.738$ (3) Å, $V = 921.1$ Å³] was determined at room temperature by single-crystal X-ray diffraction and is shown to be isostructural with KTiOPO_4 . Certain differences in the details of the crystal structures of KSP and KTP are, however, very pronounced. In particular, in KSP, the oxygen framework approximates very closely to a centrosymmetric arrangement and the Sn coordination octahedra are much less distorted than their TiO_6 counterparts so that anomalously shortened Sn—O bonds equivalent to the very short (1.716 and 1.733 Å) Ti—O bonds in KTP do not appear. The principles of bond polarizability theory and the structural data are used to correlate the structural differences between KTP and KSP with the fact that the second-harmonic generation output for KSP is only 2% of that shown by an equivalent KTP sample. The results demonstrate further proof that the short Ti—O bonds in KTP are the important structural features leading to the high optical nonlinearity of this material.

Introduction

KTiOPO_4 (KTP), orthorhombic, space group $Pna2_1$ (C_{2v}^9), lattice parameters $a = 12.819$ (3), $b = 6.399$ (1), $c = 10.584$ (2) Å ($V = 868.1$ Å³, $Z = 8$), has been of interest for some years because of its strong non-

linear optical properties (Zumsteg, Bierlein & Gier, 1976). Several structural analogues of KTP in which K is substituted by Rb, Tl (Masse & Grenier, 1971) or Na (Bamberger, Begun & Cavin, 1988) and P by As (El Brahimy & Durand, 1986) have been described. Until very recently, the only reported structural analogue of KTP in which the Ti had been substituted by another tetravalent cation was KSnOPO_4 (KSP) which was identified by Slobodyanik, Nagorny, Skopenko & Lugovskaya (1987) as a result of an investigation of $M_2\text{O}-\text{P}_2\text{O}_5-\text{SnO}_2$ ($M = \text{Li, Na, K}$) systems at 1223–1323 K. The compound was found to exist in a very narrow region of the phase diagram ($\text{K}_2\text{O}:\text{P}_2\text{O}_5$ ratios in the range 1.3–1.46) and appeared, from X-ray powder data, to be isostructural with KTP with very similar lattice parameters $a = 12.90$, $b = 6.45$ and $c = 10.50$ Å ($V = 873.65$ Å³). However, since then, Stucky, Phillips & Gier (1989) have published a review of their studies on a large number of KTP derivatives many of which have been partly or fully substituted on the Ti site.

The purpose of this study of compounds of the KTiOPO_4 family lies in the understanding of the effect that compositional modifications have on the physical properties in general and on the nonlinear optical properties (exemplified by the second-harmonic generation) in particular. KTP is a particularly efficient doubler of the Nd:YAG fundamental frequency ($\lambda = 1.06$ μm) into the green part of the optical spectrum and is an advantageous material because of its high laser-damage threshold, large temperature bandwidth for phase matching and mechanical robustness in addition to its high basic nonlinearity. The principal structural origin of the large optical nonlinearity in KTP has long been considered to be the anomalously short Ti—O bonds which give rise to highly distorted TiO_6 octahedra (Tordjman, Masse & Guitel, 1974). The effect of altering the oxygen coordination of Ti has been demonstrated by Eddy, Gier, Keder, Stucky, Cox, Bierlein & Jones (1988) in their study of inclusion-tuned KTP derivatives. Stucky *et al.* (1989) have also considered the relationship between crystal structure and nonlinear optical properties and have shown in particular that substituents on the K site may have

considerable influence on the observed second-harmonic generation. However, in KSP, only the Ti site is modified so that we shall, to a good first approximation, treat this as the site of maximum influence on the resulting optical properties.

The crystal structure of KSnOPO₄ has not been reported previously. In this study we have found that KSP is indeed a structural analogue of KTP. However, we have also measured the second-harmonic generation output power of KSP and have found it to be only about 2% of that produced by a similarly prepared sample of KTP in agreement with the findings of Jarman & Grubb (1988). The aim of this work is to explain this observation from a structural point of view with particular reference to the short Ti—O bonds occurring in the highly distorted TiO₆ octahedra of KTP. The structural refinement of KTP is reported here both for the purposes of comparison and because our refinement, which includes the Rogers (1981) polarity parameter, provides us with reliable coordinates for our structural calculations.

Experimental

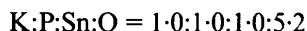
Crystals of KTP were grown from a flux using the method of Jacco, Loiacono, Jago, Mizell & Greenberg (1984). Crystals of KSP were grown by an analogous route with the TiO₂ in the starting composition substituted by SnO₂ so that the ratios of the initial materials were



by weight. The powders were mixed, placed in a platinum crucible and then heated to 1423 K. The melt was held at this temperature for 12 h and it was then cooled to room temperature at 5 K h⁻¹. The crystals which grew by spontaneous nucleation during cooling were of a KTP-like habit, of size 0.2–1 mm and slightly yellow in colour. Investigation under the polarizing microscope showed that they were generally transparent and showed sharp optical extinctions. Any flux adhering to the crystals was dissolved away in water.

KSnOPO₄ was identified using X-ray powder diffraction. The data were collected in the range 5–80° 2θ using a Stoe–Stadi 2P powder diffractometer. An autoindexing procedure gave the crystal system as orthorhombic with lattice parameters $a = 13.153$, $b = 6.532$ and $c = 10.733$ Å ($V = 921.98$ Å³) which are similar to the parameters quoted by Jarman & Grubb (1988).

Electron-probe microanalysis of the material revealed that the chemical composition was given by



showing that the phase was compositionally close to KSnOPO₄.

Table 1. *Details of data collection and crystal structure refinement for KTiOPO₄*

Crystal colour, shape and size	Colourless fragment, largest dimensions ~0.3 mm
Linear absorption coefficient (cm ⁻¹)	32.3
Diffractometer	Enraf–Nonius CAD-4
Radiation	Mo Kα
Lattice parameters from 25 reflections	$a = 12.819$ (3), $b = 6.399$ (1), $c = 10.584$ (2) Å $\alpha = 90.01$ (1), $\beta = 89.99$ (2), $\gamma = 90.03$ (2)° 0.7035
Max. (sinθ)/λ (Å ⁻¹)	–14 to 14, –1 to 9, –1 to 18
Ranges of h , k and l	Monitored every 2 h
Intensity control	Every 150 reflections
Orientation control	5578
Number of reflections measured	2158 [$F_o^2 > 3\sigma(F_o^2)$]
Number of unique observed reflections	0.0277
R_{int} *	Empirical ψ scans
Absorption correction method	1.11, 1.00
Max. and min. absorption corrections	CRYSTALS
Data reduction	Tordjman <i>et al.</i> (1974)
Model structure	<i>International Tables for X-ray Crystallography</i> (1974), neutral atoms
Atomic scattering factors, f' and f''	Full-matrix least squares (CRYSTALS)
Refinement method	Unit weights
Weighting scheme	147
Number of parameters	0.024 (0.024)
R (wR)	130 (3)
Isotropic extinction parameter†	1.08 (7)
Rogers polarity parameter	

* $R_{int} = \sum[SD(I)]/\sum[M(I)]$, where $SD(I) = \sum\langle F^2(I) \rangle - F^2(I)$ summed over J contributors $M(I) = \sum\langle F^2(I) \rangle$ summed J times.

† Larson extinction parameter (Larson, 1970).

Measurement of second-harmonic generation

The measurement of the power generated at a second-harmonic frequency by a powdered specimen of a material gives an order-of-magnitude estimate of the degree of the optical nonlinearity of the material (Kurtz & Perry, 1968). The second-harmonic generation of an unknown sample is generally compared with that of known standards. For this experiment, KTP itself was used as a standard because its similarity to KSP helped to minimize the errors inherent in the experiment. The measurements were performed using powders of both KTP and KSP sieved to grain sizes within the range 105–180 μm. The same geometry was employed for each test with the second-harmonic output power measured in a forward-scattering cone. The fundamental wavelength used was 1.06 μm produced by a Q-switched Nd:YAG laser (pulse length 30 ns at 10 Hz), as this is the wavelength at which KTP is known to respond strongly. Both the reference and second-harmonic pulses were recorded using a storage oscilloscope. The peak output of KSP was only 1/60 of the peak output of KTP which is a significant result even given the uncertainties of the method.

Data collection

KTP

The details of the data collection and refinement procedure are given in Table 1. The automatic search and indexing procedure assigned a primitive orthorhombic cell having lattice parameters $a = 12.819$ (3),

Table 2. *Structural and thermal parameters (\AA^2) for KTiOPO_4*

	<i>x</i>	<i>y</i>	<i>z</i>	U_{11}	U_{22}	U_{33}	U_{23}	U_{13}	U_{12}
K(1)	0.37807 (8)	0.7806 (1)	0.6880 (1)	0.0246 (5)	0.0122 (4)	0.0239 (4)	-0.0016 (3)	-0.0059 (4)	0.0040 (3)
K(2)	0.10526 (7)	0.6990 (1)	0.9332 (1)	0.0142 (5)	0.0212 (4)	0.0282 (4)	0.0048 (4)	0.0000 (4)	0.0051 (3)
Ti(1)	0.37290 (4)	0.5001 (1)	-0.00040 (8)	0.0075 (3)	0.0061 (2)	0.0067 (2)	-0.0009 (2)	0.0000 (3)	-0.0002 (3)
Ti(2)	0.24658 (6)	0.2695 (5)	0.74836 (9)	0.0072 (3)	0.0064 (2)	0.0062 (2)	0.0002 (3)	-0.0005 (2)	0.0000 (2)
P(1)	0.49808 (8)	0.3363 (1)	0.7397 (1)	0.0061 (4)	0.0067 (3)	0.0077 (3)	-0.0005 (4)	0.0005 (3)	-0.0003 (3)
P(2)	0.18079 (7)	0.5020 (1)	0.4872 (1)	0.0085 (4)	0.0054 (3)	0.0071 (3)	0.0005 (3)	-0.0010 (2)	-0.0001 (4)
O(1)	0.4859 (2)	0.4867 (5)	0.8497 (2)	0.009 (1)	0.012 (1)	0.012 (1)	-0.0037 (9)	0.002 (1)	-0.004 (1)
O(2)	0.5103 (2)	0.4657 (5)	0.6170 (2)	0.010 (2)	0.012 (1)	0.011 (1)	0.003 (1)	0.001 (1)	0.001 (1)
O(3)	0.4004 (2)	0.1986 (4)	0.7208 (2)	0.010 (1)	0.007 (1)	0.013 (1)	0.000 (1)	-0.0002 (9)	-0.0004 (9)
O(4)	0.5934 (2)	0.1930 (4)	0.7589 (2)	0.007 (1)	0.010 (1)	0.012 (1)	0.001 (1)	-0.001 (1)	0.0003 (9)
O(7(1))	0.2248 (2)	0.9653 (4)	0.3561 (2)	0.008 (1)	0.008 (1)	0.011 (1)	-0.0016 (9)	0.0026 (9)	-0.002 (1)
O(7(2))	0.2232 (2)	0.0413 (5)	0.6097 (2)	0.009 (2)	0.011 (1)	0.011 (1)	-0.0018 (9)	-0.0036 (9)	0.000 (1)
O(5)	0.1126 (2)	0.3106 (4)	0.4585 (2)	0.011 (1)	0.006 (1)	0.012 (1)	-0.0014 (9)	-0.001 (1)	-0.002 (1)
O(6)	0.1113 (2)	0.6918 (4)	0.5117 (3)	0.012 (1)	0.008 (1)	0.014 (1)	0.001 (1)	0.002 (1)	0.001 (1)
O(7)	0.2525 (2)	0.5402 (5)	0.3718 (2)	0.010 (2)	0.009 (1)	0.010 (1)	0.0025 (9)	0.0028 (9)	0.001 (1)
O(8)	0.2528 (2)	0.4619 (5)	0.6008 (2)	0.012 (2)	0.012 (1)	0.009 (1)	0.0035 (9)	-0.003 (1)	-0.004 (1)

$b = 6.399 (1)$ and $c = 10.584 (2) \text{\AA}$ ($V = 868.19 \text{\AA}^3$). Data were collected in the range $3\text{--}30^\circ$ in θ assuming the space group $Pna2_1$ (systematic absences were not measured). The data reduction was performed using the program *CRYSTALS* (Watkin, Carruthers & Betteridge, 1985). An empirical absorption correction was applied to the data although the effects of absorption for a sample of average dimension 0.3 mm were very small.

The refinement using the routines of *CRYSTALS* proceeded smoothly with the data refining to a final R factor of 0.025 for 2076 reflections having $I > 3\sigma(I)$. The Rogers (1981) polarity parameter refined to the value $1.08 (6)$ indicating that the crystal was of a single polarity. The structural and thermal parameters obtained are listed in Table 2.*

KSP

For details of the data collection and refinement, refer to Table 3. The automatic search and indexing procedures assigned a primitive orthorhombic unit cell having cell parameters $a = 13.145 (3)$, $b = 6.526 (2)$ and $c = 10.738 (3) \text{\AA}$ with $\alpha = \beta = \gamma = 90^\circ$ to within 0.02° . The unit-cell volume (921.15\AA^3) was of a similar size to that obtained by powder diffraction. The data were initially collected over the whole sphere in reciprocal space in order to check the assignment of the space group. Examination of the $1kl$ and $0kl$ layers showed that the unobserved reflections were consistent with the space group $Pna2_1$. The data collection was then restricted to the ranges $h = 0$ to 12 , $k = 0$ to 12 , $l = -10$ to 10 and their centrosymmetric opposites, so that at least two equivalents of a general reflection were measured.

The data reduction was performed using *CRYSTALS*. Data from ψ scans for five reflections having θ values across the measuring range were

* Lists of structure factors have been deposited with the British Library Document Supply Centre as Supplementary Publication No. SUP 52692 (26 pp.). Copies may be obtained through The Technical Editor, International Union of Crystallography, 5 Abbey Square, Chester CH1 2HU, England.

Table 3. *Details of data collection and crystal structure refinement for KSnOPO_4*

Crystal colour, shape and size	Pale-yellow prism, dimensions 0.23–0.31 mm
Linear absorption coefficient (cm^{-1})	63.69
Diffractometer	Enraf-Nonius CAD-4
Radiation	$\text{Mo K}\alpha$
Lattice parameters from 25 reflections	$a = 13.145 (3)$, $b = 6.526 (2)$, $c = 10.738 (3) \text{\AA}$ $\alpha = 89.98 (2)$, $\beta = 89.98 (2)$, $\gamma = 90.02 (2)^\circ$
Maximum $(\sin \theta)/\lambda$ (\AA^{-1})	0.7035
Ranges of h , k and l	0 to 12, 0 to 12, -10 to 10 (plus Friedel partners)
Intensity control	Four reflections hourly
Orientation control	Every 250 reflections
Number of reflections measured	4910
Number of unique observed reflections	1400 [$F_o > 6\sigma(F_o)$]
R_{int} *	0.029
Absorption correction method	Empirical ψ scans and spherical absorption ($\mu R = 0.86$)
Min. and max. absorption corrections	1.0, 1.49
Data reduction	<i>CRYSTALS</i>
Model structure	KTiOPO_4
Atomic scattering factors, f' and f''	<i>International Tables for X-ray Crystallography</i> (1974), neutral atoms
Refinement method	Full-matrix least squares (<i>SHELX76</i> and <i>CRYSTALS</i>)
Weighting scheme	$1.0419/[\sigma^2(F) + 0.0007F^2]$
R (wR)	0.021 (0.021)
Rogers polarity parameter	-0.2 (1)
Isotropic extinction parameter, χ^\dagger	0.0065 (1) (<i>SHELX76</i>)
Maximum $\Delta f/\sigma$	0.06
$\Delta\rho_{\text{max}}$, $\Delta\rho_{\text{min}}$ (e \AA^{-3})	1.43, 1.21

* R_{int} is the same as given in the footnote to Table 1.

† Isotropic extinction parameter modifies F_{calc} as follows: $F'_{\text{calc}} = F_{\text{calc}} \times (1 - 0.0001\chi F_{\text{calc}}^2/\sin \theta)$.

used to obtain an empirical absorption correction. A spherical absorption correction based on the average crystal dimension (radius 0.135 mm , $\mu R = 0.86$) was also applied. Refinements were carried out using both the routines of *CRYSTALS* and *SHELX76* (Sheldrick, 1976).

The model used for refinement was based on the KTP structure refinement reported here. The input model refined isotropically to $R = 0.026$ ($wR = 0.026$). The polarity refined to a small negative value $[-0.2 (1)]$ indicating that the polarity of the crystal was rather indeterminate and suggesting the presence of polar twins. There were some high correlations between the thermal parameters of O atoms in the pairs O(1) and O(2), O(3) and O(4), ..., O(9) and O(10). The correlation ($> 85\%$) between the parameters of O(1) and O(2) was particularly severe leading

Table 4. *Displacements of atoms in KTP and KSP from high-symmetry positions*

	Position in room-temperature structure - ($\frac{1}{4}, \frac{1}{4}, \frac{1}{4}$) for origin shift			Position in high-temperature structure (space group <i>Pnan</i>)	Displacements $\Delta x, \Delta y, \Delta z$ when <i>n</i> -glide plane is assumed to pass through (0, 0, $\frac{1}{4}$) (Å)			Displacement Δz when $\sum m_i(z_i - z_j)$ is minimized (Å)
KTP								
Ti(1)	0.1229,	0.2496,	0.7496	$\bar{x} + \frac{1}{4}, \frac{1}{4}, \frac{1}{4}$ [4(<i>d</i>) (<i>x</i> = 0.3771)]	0,	-0.002,	-0.004	-0.046
Ti(2)	0.9966,	0.0195,	0.4984	0, 0, $\frac{1}{4}$ [4(<i>b</i>)]	-0.043,	0.125,	-0.017	-0.059
K(1)	0.1281,	0.5306,	0.4380	Average (<i>x, y, z</i>) for general position 0.1364, 0.5403, 0.378	0.106,	0.062,	0.635	+0.599
K(2) (pseudo <i>n</i> glide related to K1 above)	0.6447,	0.0501,	0.1820					
P(1)	0.2481,	0.0863,	0.4897	$\frac{1}{4}, -y + \frac{1}{4}, \frac{1}{4}$ [4(<i>e</i>)]	-0.024,	0,	-0.109	-0.151
P(2)	0.9308,	0.2520,	0.2372	$x, \frac{1}{4}, \frac{1}{4}$ [4(<i>d</i>)]	0,	0.013,	-0.135	-0.178
O(1)	0.2359,	0.2367,	0.5997	Average (<i>x, y, z</i>) for general position 0.2378, 0.2262, 0.6163	0.097,	0.067,	0.176	-0.217
O(2)	0.7397,	0.7158,	0.8670					
O(3)	0.1504,	0.9486,	0.4708	0.1505, 0.9408, 0.4809	0.001,	0.050,	0.107	-0.150
O(4)	0.6506,	0.4430,	0.0089					
O7(1)	0.9748,	0.7153,	0.1061	0.9740, 0.7120, 0.1232	0.010,	0.021,	0.181	-0.223
O7(2)	0.4732,	0.2087,	0.3597					
O(5)	0.8626,	0.0606,	0.2084	0.8619, 0.0594, 0.2233	0.009,	0.001,	0.157	-0.200
O(6)	0.3613,	0.5582,	0.2617					
O(7)	0.0025,	0.2902,	0.1218	0.0026, 0.2891, 0.1355	0.001,	0.007,	0.145	-0.187
O(8)	0.5028,	0.7881,	0.3508					
KSP								
Sn(1)	0.1229,	0.2476,	0.7502	$\bar{x} + \frac{1}{4}, \frac{1}{4}, \frac{1}{4}$ [4(<i>d</i>)]	0,	-0.016,	0.002	-0.115
Sn(2)	0.9987,	0.0044,	0.4996	0, 0, $\frac{1}{4}$ [4(<i>b</i>)]	-0.017,	0.029,	-0.004	-0.117
P(1)	0.2512,	0.0911,	0.5020	$\frac{1}{4}, -y + \frac{1}{4}, \frac{1}{4}$ [4(<i>e</i>)]	0.016,	0,	0.021	-0.092
P(2)	0.9258,	0.2517,	0.2470	$x, \frac{1}{4}, \frac{1}{4}$ [4(<i>d</i>)]	0,	0.011,	-0.032	-0.145
K(1)	0.1253,	0.5271,	0.4483	0.1332, 0.542, 0.3795	0.104,	0.097,	0.739	+0.625
K(2)	0.6411,	0.0569,	0.1893					
O(1)	0.2378,	0.2383,	0.6156	0.2367, 0.2332, 0.6142	0.014,	0.033,	0.015	-0.098
O(2)	0.7356,	0.7282,	0.8871					
O(3)	0.1583,	0.9551,	0.4793	0.1584, 0.9540, 0.4779	0.001,	0.007,	0.014	-0.099
O(4)	0.6586,	0.4530,	0.0234					
OS(1)	0.9785,	0.7327,	0.1144	0.9816, 0.7243, 0.1189	0.041,	0.055,	0.048	-0.065
OS(2)	0.4847,	0.2159,	0.3766					
O(5)	0.8652,	0.0660,	0.2261	0.8613, 0.0648, 0.2264	0.051,	0.008,	0.003	-0.110
O(6)	0.3574,	0.5637,	0.2733					
O(7)	0.9950,	0.2818,	0.1343	0.9967, 0.2800, 0.1379	0.022,	0.012,	0.039	-0.074
O(8)	0.4985,	0.7782,	0.3585					

to a small isotropic U of 0.002 Å² for O(1). The same type of correlations between O atoms appeared both for data which had been treated with a spherical absorption correction and for those which had not. However, the correlations were less severe for the spherical-absorption-corrected data. Anisotropic refinement led to nonpositive definite thermal ellipsoids for six out of ten of the O atoms. Again, there was significant correlation between the U_{ij} 's for the atom pairs O(1) and O(2), O(3) and O(4), ..., O(9) and O(10). Inspection shows that the coordinates of the O atoms in the pairs above are very close to being *n*-glide related (Table 4) if a pseudo-glide plane is assumed to be perpendicular to the *c* axis at $z = 0.5$. This suggests that the room-temperature structure is a distortion from a high-temperature centrosymmetric prototype phase with space group *Pnan* (D_{2h}^6). [In order to make our origin choice for *Pnan* consistent with that of *International Tables for X-ray Crystallography*, we have origin-shifted the coordinates of all atoms by ($\frac{1}{4}, \frac{1}{4}, \frac{1}{4}$) from their room-temperature positions in preparing Table 4.] The high correlations of the thermal parameters of the O atoms probably resulted from the strong pseudo-symmetry of the oxygen framework. When the thermal parameters of pairs of O atoms were con-

strained to reflect the *n*-glide pseudosymmetry, a more rapidly converging refinement was obtained with the paired thermal parameters refining to reasonable values similar to those obtained for KTP in which no correlation problems occurred. The pairs of O atoms in KTP are not as closely pseudo-*n*-glide-related (Table 4) and so correlation effects are not as prominent. The constrained refinement was taken as the best result. The positional and thermal parameters are listed in Table 5 and the bond lengths are given in Table 6.*

Discussion

The structural studies have shown that KSP is a direct structural analogue of KTP. However, there are some important differences which have a significant effect on the nonlinear optical properties, particularly when the SnO₆ and TiO₆ octahedra are compared. Although the crystal structure of KTP has been well known for some time, certain of its features have not been commented upon before. These have become much more apparent on comparing KTP with the crystal structure of the analogous compound KSP.

* See deposition footnote.

Table 5. Atomic coordinates and thermal parameters (\AA^2) for KSnOPO_4

	<i>x</i>	<i>y</i>	<i>z</i>	U_{11}	U_{22}	U_{33}	U_{23}	U_{13}	U_{12}
K(1)	0.3753 (1)	0.7771 (2)	0.6983 (0)	0.0171 (9)	0.0089 (7)	0.0243 (8)	-0.0003 (6)	-0.0038 (5)	0.0050 (7)
K(2)	0.1089 (1)	0.6930 (3)	0.9393 (2)	0.0126 (8)	0.0210 (7)	0.0307 (8)	0.0001 (8)	0.0001 (6)	0.0063 (7)
Sn(1)	0.2487 (0)	0.2544 (1)	0.7496 (2)	0.0025 (2)	0.0033 (2)	0.0038 (2)	-0.0003 (1)	-0.0006 (1)	-0.0004 (1)
Sn(2)	0.3729 (0)	0.4976 (1)	0.0002 (2)	0.0028 (2)	0.0019 (2)	0.0036 (2)	-0.0006 (1)	-0.0003 (3)	0.0003 (2)
P(1)	0.5012 (1)	0.3411 (2)	0.7520 (3)	0.0033 (8)	0.0049 (6)	0.0057 (5)	-0.003 (1)	0.0012 (4)	0.0004 (8)
P(2)	0.1758 (1)	0.5017 (3)	0.4970 (4)	0.0038 (8)	0.0030 (6)	0.0062 (5)	0.0005 (6)	-0.004 (1)	-0.0014 (8)
O(1)	0.4878 (6)	0.4883 (7)	0.8656 (6)	0.009 (1)	0.009 (1)	0.010 (1)	-0.0029 (9)	0.0037 (8)	-0.004 (1)
O(2)	0.9856 (6)	0.9782 (7)	0.1371 (6)	0.009 (1)	0.009 (1)	0.010 (1)	0.0029 (9)	-0.0037 (8)	-0.004 (1)
O(3)	0.4083 (4)	0.2051 (7)	0.7293 (4)	0.002 (1)	0.010 (1)	0.014 (1)	-0.003 (1)	-0.0022 (8)	0.001 (1)
O(4)	0.9086 (4)	0.7030 (7)	0.2734 (4)	0.002 (1)	0.010 (1)	0.014 (1)	0.003 (1)	0.0022 (8)	0.001 (1)
O(5)	0.1062 (4)	0.3160 (6)	0.4761 (4)	0.011 (1)	0.007 (1)	0.008 (1)	-0.001 (1)	-0.0031 (7)	0.000 (1)
O(6)	0.6074 (4)	0.8137 (7)	0.5233 (4)	0.011 (1)	0.007 (1)	0.008 (1)	0.001 (1)	0.0031 (7)	0.000 (1)
OS(1)	0.2285 (6)	0.9827 (8)	0.3644 (6)	0.009 (1)	0.007 (1)	0.011 (1)	-0.002 (1)	-0.0048 (8)	0.000 (1)
OS(2)	0.7347 (6)	0.4659 (9)	0.6266 (6)	0.009 (1)	0.007 (1)	0.011 (1)	0.002 (1)	-0.0048 (8)	0.000 (1)
O(7)	0.2450 (5)	0.5318 (9)	0.3843 (7)	0.010 (1)	0.012 (1)	0.012 (1)	0.006 (1)	0.0033 (8)	0.002 (1)
O(8)	0.7485 (5)	0.0282 (9)	0.6085 (7)	0.010 (1)	0.012 (1)	0.012 (1)	-0.006 (1)	-0.0033 (8)	0.002 (1)

Table 6. Bond lengths (\AA) in KSnOPO_4

Sn(2)O ₆ octahedron		Sn(1)O ₆ octahedron	
Sn(2)—O(1)	2.091 (7)	Sn(1)—O(3)	2.134 (5)
Sn(2)—O(2)	2.093 (7)	Sn(1)—O(4)	2.102 (5)
Sn(2)—OS(1)	1.978 (6)	Sn(1)—OS(1)	1.957 (5)
Sn(2)—OS(2)	1.975 (7)	Sn(1)—OS(2)	1.961 (5)
Sn(2)—O(5)	2.111 (6)	Sn(1)—O(7)	2.051 (6)
Sn(2)—O(6)	2.064 (5)	Sn(1)—O(8)	2.076 (7)
O(1)—O(2)	2.923 (6)	O(3)—OS(1)	2.937 (7)
O(1)—O(5)	2.740 (7)	O(3)—OS(2)	2.767 (6)
O(1)—O(6)	2.884 (8)	O(3)—O(7)	2.848 (7)
O(1)—OS(1)	2.843 (8)	O(3)—O(8)	3.021 (9)
O(2)—OS(2)	2.899 (9)	O(4)—OS(1)	2.834 (8)
O(2)—O(5)	2.850 (7)	O(4)—OS(2)	2.995 (8)
O(2)—O(6)	2.790 (7)	O(4)—O(7)	3.006 (9)
OS(1)—O(5)	2.958 (9)	O(4)—O(8)	2.949 (7)
OS(1)—OS(2)	2.838 (8)	O(7)—OS(1)	2.959 (7)
OS(2)—O(6)	3.031 (8)	O(7)—OS(2)	2.779 (9)
OS(2)—O(5)	2.974 (9)	O(8)—OS(1)	2.764 (8)
OS(1)—O(6)	3.032 (9)	O(8)—OS(2)	2.869 (6)
P(1)O ₄ tetrahedron		P(2)O ₄ tetrahedron	
P(1)—O(1)	1.562 (6)	P(2)—O(5)	1.535 (5)
P(1)—O(2)	1.535 (7)	P(2)—O(6)	1.529 (6)
P(1)—O(3)	1.530 (5)	P(2)—O(7)	1.527 (8)
P(1)—O(4)	1.506 (6)	P(2)—O(8)	1.545 (7)
O(1)—O(2)	2.480 (7)	O(5)—O(6)	2.469 (8)
O(1)—O(3)	2.579 (8)	O(5)—O(7)	2.508 (7)
O(1)—O(4)	2.510 (8)	O(5)—O(8)	2.560 (8)
O(2)—O(3)	2.471 (6)	O(6)—O(7)	2.553 (6)
O(2)—O(4)	2.529 (7)	O(6)—O(8)	2.497 (7)
O(3)—O(4)	2.453 (7)	O(7)—O(8)	2.441 (6)
K(1)O ₈ cage		K(2)O ₈ cage	
K(1)—O(1)	2.995 (7)	K(2)—O(1)	2.736 (6)
K(1)—O(2)	2.753 (4)	K(2)—O(2)	3.256 (8)
K(1)—O(3)	2.845 (5)	K(2)—O(4)	3.148 (5)
K(1)—OS(1)	2.955 (5)	K(2)—OS(1)	2.664 (5)
K(1)—OS(2)	2.611 (6)	K(2)—OS(2)	3.058 (7)
K(1)—O(5)	3.005 (4)	K(2)—O(5)	2.856 (6)
K(1)—O(7)	3.042 (4)	K(2)—O(7)	2.987 (6)
K(1)—O(8)	2.770 (7)	K(2)—O(8)	3.182 (7)
		K(2)—O(3)	3.123 (7)

Pseudosymmetry and the prototype phase

The most notable property of both crystal structures is their exhibition of a strong pseudosymmetry which was mentioned earlier in connection with the oxygen framework in KSP and which can be identified similarly in KTP. This led us to postulate *Pnan* symmetry for the structure of the prototype phase in conflict with the statements of some other workers (Yanovskii & Voronkova, 1980). High-temperature high-resolution neutron powder diffraction on KTP

has been undertaken to confirm our predictions and Rietveld refinement of the results is currently underway. However, since the completion of the work presented here, Harrison, Gier, Stucky & Schultz (1989) have studied the phase transition in TiTiOPO_4 and have solved the high-temperature structure in space group *Pnan* (D_{2h}^6). The discussion which follows is concerned both with the relationship between the room-temperature and high-temperature phases of KTP and KSP and with the pseudosymmetry inherent in the KTP structure. Since the structural details of the work of Harrison *et al.* are not available at the time of writing, we cannot as yet compare our model with their experimental findings.

The closeness to *n*-glide symmetry noted for the oxygen framework holds also for the cations in both KTP and KSP. Special position sites for the cations Ti/Sn and P in the hypothetical prototype phase (space group *Pnan*) can easily be identified from the room-temperature positions (Table 4). Placing the K ions in the high-temperature structure of KTP, for example, is less straightforward. If they are placed on special positions, then the displacements calculated are particularly large in the *a* and *b* directions *e.g.* K(1) at (0.1281, 0.5306, 0.4380) on special position (0, $\frac{1}{2}$, $\frac{1}{2}$) [4(*a*)] leads to $\Delta x = 1.642 \text{ \AA}$, K(2) at (0.8553, 0.4490, 0.6832) on (x , $\frac{1}{4}$, $\frac{3}{4}$) [4(*d*)] leads to $\Delta y = 1.275 \text{ \AA}$ or on ($\frac{3}{4}$, $y + \frac{1}{2}$, $\frac{1}{2}$) [4(*c*)] leads to $\Delta x = 1.350 \text{ \AA}$. The Δz 's corresponding to K(1) on 4(*a*) and K(2) on 4(*d*) are -0.656 and -0.707 \AA respectively which are within the 1 \AA limit set by Abrahams (1988) for displacements along the polar axis associated with a paraelectric/ferroelectric phase transition. The displacements of the K atoms in all directions can, however, be reduced if a different model in which the K(1) and K(2) sites are considered to be a pseudo-*n*-glide-related pair of the same type as the pairs of O atoms considered earlier. In this description, the Δx 's and Δy 's of the K atoms are considerably reduced (Table 4) and the Δz for each K atom decreases to 0.635 \AA . (We note here that Harrison *et al.* quote TI displacements of about 0.7 \AA in going

from the room-temperature to the high-temperature phase.) Therefore, in the second model, even the *sign* of the Δz 's for the K atoms reverses. Such a sign change is significant in the study of the relationship between polar properties and crystal structure.

Evidence for the suggested prototype structure described by the second model is provided by the program *MISSYM1.1* (Le Page, 1988) which searches given atomic arrangements for 'unseen' pseudosymmetry relationships subject to user-specified tolerances. The results of the *MISSYM* runs on the KTP and KSP structures are summarized in Table 7. The following points should be noted:

(i) When the K atoms are excluded from the crystal structures of KTP and KSP, the resulting Ti—O—P and Sn—O—P frameworks show very close pseudocentrosymmetry accompanied by *n*-glide symmetry. The pseudosymmetry is more closely obeyed in KSP than in KTP.

(ii) When the K atoms are included in the crystal structures, much larger tolerances must be specified in order to obtain the same pseudosymmetry relationships confirming that the K atoms are those deviating furthest from the prototype phase positions.

(iii) When each of K(1) and K(2) is excluded in turn from the crystal structures, the pseudosymmetry relationships cannot be found in the remaining atomic arrangements indicating that the K atoms are pseudosymmetrically related to each other rather than lying close to special positions in the prototype phase.

(iv) In support of our assertion that the prototype symmetry may well be *Pnan* rather than *Pnam*, a mirror plane relationship between the atoms in either structure is not found even at very high tolerances.

The program *MISSYM* finds that the *n*-glide plane passes through Ti(1) in KTP or through Sn(1) in KSP. As the *z* coordinate of the origin is not fixed in the polar space group *Pna2*₁, we can choose the 'best' position for the *n*-glide plane in the prototype structure. The most physically reasonable position should be at that *z* coordinate which minimizes the sum of the weighted displacements from the high-temperature positions of all atoms in the structure. The quantity minimized is $\sum_i m_i(z_i - z_n)$, where m_i is the atomic mass of the *i*th atom, z_i is the displacement of the *i*th atom from its high-temperature position, assuming that the glide plane passes through $z = 0.25$ (fourth column of Table 4) and z_n is a variable increment. The result of the minimization is that the best position for the glide plane is at $z = 0.2541$ in KTP (using the *Pnan* origin) and at $z = 0.2606$ in KSP.

The spontaneous polarization developed in the room-temperature phase can now be calculated from

Table 7. Results from the program *MISSYM1.1*

Crystal structure input to <i>MISSYM1.1</i>	Tolerance distance to average position for pseudosymmetry plane/inversion centre (Å)
KTP structure excluding K atoms	0.19
KSP structure excluding K atoms	0.10
KTP structure (K atoms included)	0.66
KSP structure (K atoms included)	0.76
KTP structure excluding either K(1) or K(2)	No pseudosymmetry detected (tolerance > 2.0 Å)
KSP structure excluding either K(1) or K(2)	No pseudosymmetry detected (tolerance > 2.0 Å)

The symmetry elements detected are: (1) for KTP - *n*-glide plane \perp' [001] through (0, 0, 0), inversion centre at (0.25, 0.25, 0.75); (2) for KSP - *n*-glide plane \perp' [001] through (0, 0, 0.008) inversion centre at (0.25, -0.252, 0.258) where 0.008 is the *z* coordinate of Sn(1).

our model of the prototype phase. This is achieved by use of a simple point-charge model in which \mathbf{P}_s is given by

$$\mathbf{P}_s = (1/V) \sum_i q_i \Delta z_i$$

where V is the unit-cell volume, q_i is the charge on the *i*th atom (assumed to be the full ionic charge) and Δz_i is the displacement along the polar axis of the *i*th atom from its room-temperature position to its position in the high-temperature centrosymmetric phase (the structural arrangement in which $\mathbf{P}_s = 0$). Using the Δz 's listed in the final column of Table 4, we obtain a spontaneous polarization of 0.224 C m^{-2} directed parallel to $+\mathbf{c}$ as shown in Fig. 1. The magnitude of \mathbf{P}_s is close to that calculated by Bierlein & Arweiler (1986) who predicted the value 0.19 C m^{-2} from electrooptical data and the value 0.24 C m^{-2} from a point-charge model. In the latter, they did not specify their choice of centrosymmetric prototype and they considered cation displacements only; therefore, we cannot make a significant comparison between their calculation and ours. We have also calculated the spontaneous polarization developed in KSP and found that it is significantly smaller (0.07 C m^{-2}) than that of KTP, as expected.

In our model, the displacements (Fig. 1) of all but the K atoms are in the same sense, *i.e.* antiparallel with the chosen sense of $+\mathbf{c}$. The severe shortening of one of the Ti—OT bonds in each of the TiO₆ octahedra occurs because the displacements of the OT atoms (0.223 Å) far exceed the Ti displacements (0.046 and 0.059 Å). Therefore, as OT(1), Ti(2) and OT(2), for example, move in the same sense along the polar axis, the OT(1)—Ti(2) bond is forced to contract and the Ti(2)—OT(2) bond to extend. The magnitude of the contraction/extension, 0.164 Å , is given by the difference of the OT displacement and the Ti(2) displacement. Therefore, our model predicts that the long and short bonds of the Ti(2)O₆ octahedron should differ in length by $2 \times 0.164 = 0.328 \text{ Å}$, whereas the real difference is 0.359 Å . Similarly, the model predicts a bond-length difference of 0.348 Å for the pair of bonds Ti(1)—O(1) and

Ti(1)—OT(2) in the Ti(1)O₆ octahedron which does not match the real value (0.434 Å). Therefore, this model cannot account completely for the high distortions found in the TiO₆ octahedra at room temperature.

Crystal structures

In KTP, the bond lengths in the TiO₆ octahedra range between 1.716 and 2.150 Å [Ti(1)O₆] and 1.733 and 2.092 Å [Ti(2)O₆]. We can measure the distortion of the octahedra by finding the mean *M*—O bond lengths and then calculating the average deviations from the means [*i.e.* $(\sum_i^6(x_i - \bar{x}))/6$]. For the TiO₆ octahedra in KTP the mean Ti—O bond lengths are 1.972 and 1.967 Å with respective average deviations from the means of 0.143 and 0.122 Å, whereas for the SnO₆ octahedra in KSP the mean Sn—O bond lengths are 2.052 and 2.047 Å with respective average deviations of 0.06 and 0.074 Å. The lower average deviations for the Sn—O bond lengths show that the Sn atoms are not displaced much from the centres of their coordination octahedra. This indicates that the oxygen framework in KSP is closer to a centrosymmetric arrangement.

The MO₆ octahedra are corner-linked to form chains which zig-zag through the crystal structures (Figs. 2*a-d*). The O atoms which form the links in KTP are the OT(1) and OT(2) atoms which are involved in the anomalously short Ti—O bonds. [In KSP, the analogous atoms OS(1) and OS(2) link the chains.] The sequence of Ti—O bond lengths in KTP is then alternately long—short—long—short ... whereas

in KSP the Sn—O bond lengths are equalized. The displacement of the Ti atoms parallel to the polar axis can be seen clearly in the simplified Figs. 2(*a*) and 2(*b*). Note from the thermal ellipsoids for OT(1) and OT(2) that the major axes lie approximately perpendicular to the directions of the strongest bonds (the short Ti—O bonds), as expected, so that the major component of vibration tends to be parallel to the polar axis. Although not shown in the figure, in both KSP and KTP, the K atoms also exhibit highly anisotropic vibrations parallel to [001]. KTP shows considerable ionic conductivity in this direction because of the movement of K ions along the 'channels' of the crystal structure. The large magnitudes of the thermal coefficients and the anisotropy of the thermal vibration ellipsoids is consistent with this behaviour.

Although the Ti—O bonding sequence in the chains contains the anomalously short bonds Ti(1)—OT(2) and Ti(2)—OT(1), it only contains one of the correspondingly long bonds, *i.e.* Ti(2)—OT(2) (2.092 Å). This results from the chain turning through a right-angle [OT(1)—Ti(1)—OT(2) = 94.82°] at Ti(1) so that the other long bond [Ti(1)—OT(1) = 2.150 Å] occurring 'opposite' to Ti(1)—OT(2) in the octahedron is not used in chain formation. [The O(1) atom is shared with the P(1)O₄ tetrahedron and is therefore not available to corner-link the octahedron.] The effect of the 90° turn is to link the TiO₆ octahedra with their equatorial planes almost perpendicular — Ti(1)O₆ is oriented with its equatorial plane almost parallel to (100) whereas that of Ti(2)O₆ is almost parallel to (010). Analogous octahedra are found in KSP.

The tendency for Sn coordination to be less distorted than that for Ti is also seen when the structures of sphene, CaTiOSi₄ (Speer & Gibbs, 1976) and malayaite, CaSnOSi₄ (Higgins & Ribbe, 1977) are considered. In CaTiOSi₄, the TiO₆ octahedra are strongly distorted again with a very short (1.766 Å) Ti—O bond. However, in CaSnOSi₄ the octahedral distortion is eliminated because the Sn atom is not displaced from the centre of the octahedron. This results in equal Sn—O bond lengths and in an additional *A*-face centring in CaSnOSi₄ (space group *A2/a*) when compared with CaTiOSi₄ (space group *P2₁/a*). It is instructive to note that malayaite is the only known structural analogue of sphene in which the Ti site is fully substituted by another cation, thus showing that there is a tendency for Sn and Ti compounds to form similar structures. The average Sn—O bond length in CaSnOSi₄ (2.042 Å) agrees well with those values found in this study (2.042 and 2.052 Å). In further support of our observations, the difference in the average *M*—O distances for the MO₆ octahedra in KTP and KSP, which are 0.08 and 0.075 Å, are found to be close to

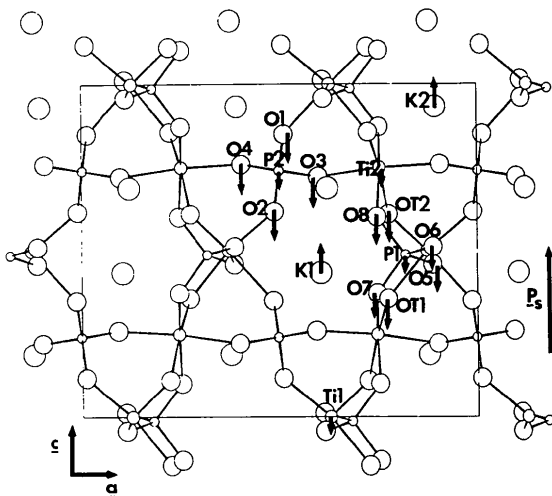


Fig. 1. A view of the KTP structure seen along [010] showing the directions for the calculated displacements of all atomic species in the transition from the prototype phase to the room-temperature phase. The direction of the resultant spontaneous polarization, *P_s*, is shown parallel with the chosen direction of +*c*.

the difference in the ionic radii (Shannon & Prewitt 1969) for Sn and Ti (0.085 Å), as expected.

The structural differences between KSP and KTP caused by the SnO₆ octahedra must have an effect elsewhere. Most obviously, we note an increase in the unit-cell volume brought about by the substitution of Ti by a larger cation having a considerably

larger average *M*—O bond length. The increase in *M*—O bond length is accommodated first by the PO₄ tetrahedra which have a greater range of bond lengths and angles than in KTP and are thus slightly more distorted. The most pronounced changes occur for those bonds which occur in the SnO₆—PO₆ chains parallel to [100] (Fig. 1) (note that the *a* lattice

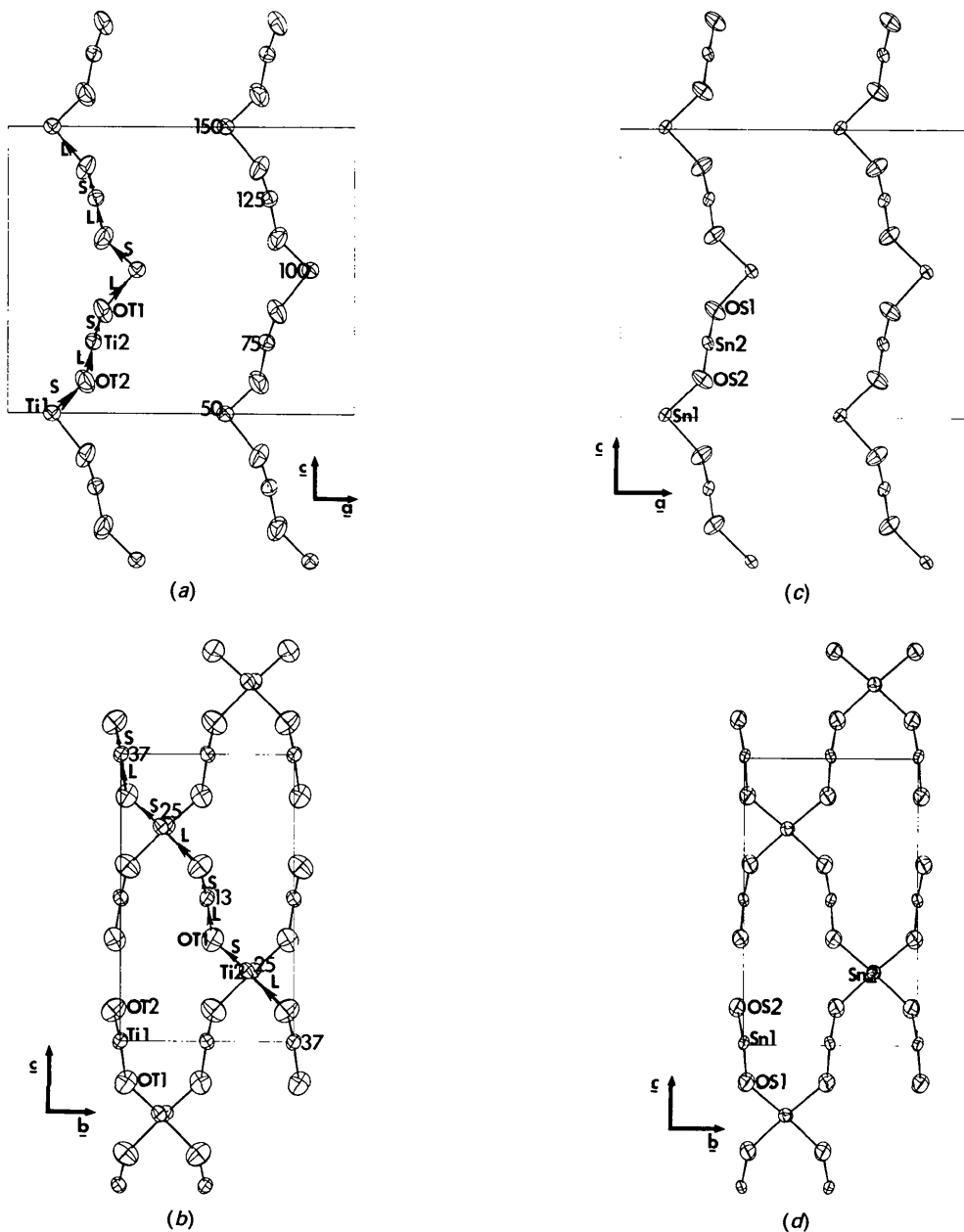


Fig. 2. (a) A view along [010] of the thermal ellipsoids (at 70% probability level) of the Ti and OT atoms only showing the formation of the Ti—OT chains in the KTP structure. The 'long' and 'short' Ti—OT bonds are denoted by L and S respectively and the heights of the atoms are marked in units of $z/c \times 100$. (b) The same atoms as in (a) but seen along [100]. The 'zig-zag' path of the Ti—OT chains is very apparent from this viewpoint. (c) A view along [010] of the Sn—OS chains in KSP [drawn to the same scale as (a)]. Long and short Sn—OS bonds equivalent to the L and S Ti—OT bonds do not appear in the chains which are otherwise analogous to those in KTP. (d) Thermal ellipsoids for the Sn and OS atoms seen along [100] [equivalent to (b) for KTP].

parameter shows the largest percentage increase). The average P—O distances in the tetrahedra (1.538 and 1.531 Å) become correspondingly shorter than those in KTP (both 1.542 Å) as the M—O bonds to the shared O atoms lengthen. Finally, the changes in the M—O and P—O bond lengths compared with those in KTP are accommodated in the KO_8 and KO_6 coordination polyhedra which show a much wider spread of bond lengths. The average K—O contact lengths (2.874 and 3.000 Å) increase relative to KTP in each of the polyhedra because these are now edge-shared with the coordination octahedra of a larger cation (Sn). As the K atoms are known to be mobile in the KTP structure, it is to be expected that the changes caused by the more strongly bound elements of the structure in KSP will eventually be taken up by the relatively loosely bound K atoms in their irregular cages.

Crystal structure and nonlinear optical properties

The relationship between optical nonlinearity and crystal structure may be established using bond-polarizability theory (Levine, 1973a). In this approach, one has to decide on the relative magnitudes of the bond polarizabilities. These will depend on various factors such as how much mobile charge is located in the bonding region, the degree of ionicity of the bond, the nature of the atoms forming the bond, *etc.* In KTP, the major contributors to the optical nonlinearity have long been considered (Zumsteg *et al.*, 1976) to be the anomalously short Ti—O bonds in the TiO_6 octahedra. Hansen, Protas & Marnier (1988) used high-precision X-ray diffraction to show that there is a build-up of charge density in the short Ti—O bonds. This observation justified their treatment of these two short bonds as a distinct bond-type having a higher bond polarizability (p^b) than the four medium-length Ti—O bonds per octahedron (the two 'long' Ti—O bonds were neglected). Since then, Stucky *et al.* (1989) have shown that M—O ($M = \text{Ti}, \text{Ge}$ and others) bonds do not account exclusively for the nonlinear optical response of KTP and its analogues. However, for the purposes of the comparison of the nonlinear optical response from KSP and KTP, we shall take the MO_6 octahedra as our starting point.

From the powder measurement on KSP, it is clear that its second-harmonic generation is much weaker than that of KTP. This measurement, all other experimental quantities being equal, effectively gives an estimate of the quantity $d^2/n(2\omega)n^2(\omega)$ where d is the average coefficient describing the second-harmonic generation from the powder and $n(2\omega)$ and $n(\omega)$ are the refractive indices at the doubled and fundamental frequencies respectively. Hence, if refractive-index differences between KSP and KTP

are negligible, the measurements indicate that d_{KSP} is of order $0.1 \times d_{\text{KTP}}$. However, in general the bond polarizabilities/optical susceptibilities for Sn—O bonds are expected to be lower than those for Ti—O bonds in respect of both linear (refractive indices) and nonlinear optical properties because the electronic configuration of Sn does not enable the enhancement of optical response which is derived from the participation of transition metal d electrons in Ti—O bonds (Levine, 1973b). In agreement with this general observation, it is noted that the substitution of Ti by Sn in the rutile crystal structure leads to considerably lower refractive indices for cassiterite, SnO_2 (Deer, Howie & Zussman, 1966) than for isostructural TiO_2 . The assumption that refractive indices of KSP are lower than those of KTP implies that d_{KSP} is even smaller than the value of $0.1 \times d_{\text{KTP}}$ which was derived from the second-harmonic generation measurement on the basis of unchanged refractive indices.

The geometrical properties of the structure arrangement are entered into the calculation of nonlinear tensor coefficients through products of direction cosines for the participating bonds. Briefly summarized, a tensor component of the second-order susceptibility is given by

$$\mathbf{d}_{ijk} = \sum_b^{\text{cell}} g_{ijk}^b p^b / V \quad (1)$$

where V is the unit-cell volume, p^b is the longitudinal bond polarizability of the b th bond (transverse component set to zero) and the g_{ijk}^b term for a bond is given by

$$g_{ijk}^b = \cos(\nu_i)\cos(\nu_j)\cos(\nu_k) \quad (2)$$

where the direction cosines are calculated with respect to global axes (here, the crystal axes).

The materials KTP and KSP are structural analogues and therefore, many of the g_{ijk}^b terms for the individual bonds are very similar. However, in forming the summations over the g_{ijk}^b for the Sn—O bonds, there is close cancellation of matching pairs of bonds quasisymmetrically placed with respect to the pseudo- n -glide plane. These pairs of bonds have almost equal and opposite values of $\cos \nu_3$ which expresses the orientation of a bond with respect to the polar axis. Hence, if all Sn—O bonds are included in the summation with equal bond polarizabilities, the geometry of KSP dictates that a high degree of cancellation occurs for all three non-zero \mathbf{d}_{ijk} coefficients \mathbf{d}_{113} , \mathbf{d}_{223} and \mathbf{d}_{333} .

By contrast, in KTP there is a strong inherent asymmetry by virtue of the presence of anomalously short and long Ti—O bonds in each highly distorted TiO_6 octahedron. Hansen *et al.* (1988) exploited this by performing intrinsically asymmetric summations involving only five out of the six Ti—O bonds per octahedron (omitting the 2.150 and 2.094 Å bonds)

and singling out the anomalously short Ti—O bonds as higher contributors. In this approach, the tensor component d_{333} is given by a two-term equation of the type

$$d_{333} = [-2.34p^{(1)} + 1.64p^{(2)}]/V_{KTP} \quad (3)$$

where $p^{(1)}$ and $p^{(2)}$ refer to the bond polarizabilities of the short- and medium-length Ti—O bonds respectively, neglecting P—O bonds. As $p^{(1)}$ is assumed to be much greater than $p^{(2)}$, there is still a large net negative effect resulting from (3) [using the experimentally measured values of the single-crystal d_{ijk} , Hansen *et al.* (1988) calculated $p^{(1)} = 14 \times p^{(2)}$]. In KSP, when all Sn—O bonds are included with equal polarizability, d_{333} is given by

$$d_{333} = (0.612p^{KSP})/V_{KSP}.$$

Assuming p^{KSP} to be approximately the same magnitude as $p^{(2)}$ in (3), the calculation indicates clearly that the expected d_{333} for KSP is considerably smaller than the KTP value. Similar relationships hold for the other non-zero tensor coefficients.

In concluding this discussion, it should be noted that the calculations from the KSP crystal structure indicate an even lower second-harmonic generation compared with KTP than the weak signal observed experimentally. However, several points should be made about the limitations of the method *i.e.*,

(i) The powder second-harmonic generation method gives, at best, order of magnitude information. Single-crystal measurements are required to investigate the structure–property relationships in detail.

(ii) It is an over-simplification to assume that all Sn—O bond polarizabilities are equal so that the cancellation of the bond contributions in the summation is overestimated here.

(iii) The contributions of the more-distorted PO₄ tetrahedra in KSP have been neglected. The increased contribution from these will tend to raise d_{KSP} .

(iv) The use of the bond-polarizability model for KTP by Hansen *et al.* (1988) was suitable because of the extreme asymmetry of the TiO₆ octahedra which allowed them to focus on specific Ti—O bonds. In a material such as KSP, the origin of the small existing nonlinear optical effect is a more subtle addition of minor contributions which is difficult to quantify in this way.

Concluding remarks

Our investigation of KSP has shown that its structure is much closer to our model of the centrosymmetric prototype than that of KTP. In particular, in the room-temperature structure, the extreme distortions characterizing the TiO₆ octahedra in KTP

are eliminated so that short Sn—O bonds equivalent to the anomalously short Ti—O bonds in KTP do not appear. This observation has been correlated with the weaker second-harmonic generation observed experimentally which has, to some extent, been modelled from the crystal structure.

The point group *mm2* which characterizes the room-temperature structure of both KTP and KSP allows them, in principle, to exhibit ferroelectricity. However, so far, a ferroelectric response in KTP has not been demonstrated by dielectric hysteresis and switching behaviour because the ionic conductivity of the material at elevated temperatures prohibits the achievement of the necessary coercive field (Bierlein & Arweiler, 1986). Dielectric experiments (Yanovskii & Voronkova, 1980) have shown that KTP undergoes a second-order phase transition at about 1207 K which they interpreted as the transition to a prototype centrosymmetric phase with the suggested space group *Pnam* (D_{2h}^1). However, our study of pseudosymmetry in the room-temperature structure has led us to believe for some time that the high-temperature structure is likely to have symmetry *Pnan* (D_{2h}^6). In support of our belief, Harrison *et al.* (1989) have recently shown that the KTP analogue TiTiOPO₄ does indeed undergo a structural phase transition from the room-temperature structure to a structure described by *Pnan* symmetry at high temperature.

References

- ABRAHAMS, S. C. (1988). *Acta Cryst.* **B44**, 585–595.
 BAMBERGER, C. E., BEGUN, G. M. & CAVIN, O. B. (1988). *J. Solid State Chem.* **73**, 317–324.
 BIERLEIN, J. D. & ARWEILER, C. B. (1986). *Appl. Phys. Lett.* **49**(15), 917–919.
 DEER, W. A., HOWIE, R. A. & ZUSSMAN, J. (1966). *An Introduction to the Rock-Forming Minerals*. London: Longman.
 EDDY, M. M., GIER, T. E., KEDER, N. L., STUCKY, G. D., COX, D. E., BIERLEIN, J. D. & JONES, G. (1988). *Inorg. Chem.* **27**(11), 1856–1858.
 EL BRAHIMI, M. & DURAND, J. (1986). *Rev. Chim. Miner.* **23**, 146–153.
 HANSEN, N. K., PROTAS, J. & MARNIER, G. (1988). *C. R. Acad. Sci.* **307**(II), 475–479.
 HARRISON, W. T. A., GIER, T. E., STUCKY, G. D. & SCHULTZ, A. J. (1989). *Am. Crystallogr. Assoc. Abstr. Ser. 2*, **17**, 103.
 HIGGINS, J. B. & RIBBE, P. H. (1977). *Am. Mineral.* **62**, 801–806.
International Tables for X-ray Crystallography (1974). Vol. IV. Birmingham: Kynoch Press. (Present distributor Kluwer Academic Publishers, Dordrecht.)
 JACCO, J. C., LOIACONO, G. M., JAGO, M., MIZELL, G. & GREENBERG, B. (1984). *J. Cryst. Growth*, **70**, 484–490.
 JARMAN, R. H. & GRUBB, S. G. (1988). *Proc. SPIE Conf. Ceram. Inorg. Cryst. Opt. Electroopt. Nonlinear Convers.* pp. 108–111.
 KURTZ, S. K. & PERRY, T. T. (1968). *J. Appl. Phys.* **39**(8), 3798–3813.
 LARSON, A. C. (1970). *Crystallographic Computing*, edited by F. R. AHMED, pp. 209–213. Copenhagen: Munksgaard.
 LE PAGE, Y. (1988). *J. Appl. Cryst.* **21**, 983–984.
 LEVINE, B. F. (1973a). *Phys. Rev. B*, **7**(6), 2600–2626.
 LEVINE, B. F. (1973b). *Phys. Rev. B*, **7**(6), 2591–2600.

- MASSE, R. & GRENIER, J. (1971). *Bull. Soc. Fr. Mineral. Cristallogr.* **94**, 437–442.
- ROGERS, D. (1981). *Acta Cryst.* **A37**, 734–741.
- SHANNON, R. D. & PREWITT, C. T. (1969). *Acta Cryst.* **B25**, 925–946.
- SHELDRIK, G. M. (1976). *SHELX76*. Program for crystal structure determination. Univ. of Cambridge, England.
- SLOBODYANIK, N. S., NAGORNYI, P. G., SKOPENKO, V. V. & LUGOVSKAYA, E. S. (1987). *Russ. J. Inorg. Chem.* **32**(7), 1023–1026.
- SPEER, J. A. & GIBBS, G. V. (1976). *Am. Mineral.* **61**, 238–247.
- STUCKY, G. D., PHILLIPS, M. L. F. & GIER, T. E. (1989). *Chem. Mater.* **1**(5), 492–509.
- TORDJMAN, I., MASSE, R. & GUITEL, J. C. (1974). *Z. Kristallogr.* **139**, 103–115.
- WATKIN, D. J., CARRUTHERS, J. R. & BETTERIDGE, P. W. (1985). *CRYSTALS User Guide*. Chemical Crystallography Department, Univ. of Oxford, England.
- YANOVSKII, V. K. & VORONKOVA, V. I. (1980). *Phys. Status Solidi a*, **93**, 665–668.
- ZUMSTEG, F. C., BIERLEIN, J. D. & GIER, T. E. (1976). *J. Appl. Phys.* **47**(11), 4980–4985.

Acta Cryst. (1990). **B46**, 343–347

Electron Density Distribution in Crystals of Sodium Nitrite at 120 K

BY MASAMI OKUDA, SHIGERU OHBA AND YOSHIHIKO SAITO*

Department of Chemistry, Faculty of Science and Technology, Keio University, Hiyoshi 3, Kohoku-ku, Yokohama 223, Japan

TETSUZO ITO

Department of Chemical Technology, Kanagawa Institute of Technology, Atsugi 243–02, Japan

AND IWAO SHIBUYA

Research Reactor Institute, Kyoto University, Kumatori, Sennan-gun, Osaka 590–04, Japan

(Received 16 January 1990; accepted 25 January 1990)

Abstract

The electron density distribution in crystals of ferroelectric sodium nitrite has been determined on the basis of the intensity data collected at 120 K. NaNO_2 , $M_r = 69.0$, orthorhombic, $Im2m$, $a = 3.518$ (1), $b = 5.535$ (1), $c = 5.382$ (1) Å, $V = 104.8$ (1) Å³, $Z = 2$, $\text{Mo } K\alpha_1$, $\lambda = 0.7093$ Å, $\mu = 0.365$ mm⁻¹, $F(000) = 68$, final $R = 0.013$ for 437 observed unique reflections after the multipole refinement. The N—O bonding electron and the lone-pair electrons of N and O atoms corresponding to sp^2 hybridization are clearly observed. The effective charges for N and O atoms were estimated to be -0.18 (10) and -0.41 (5) e, respectively. The results are compared with those for $\text{LiNO}_2 \cdot \text{H}_2\text{O}$.

Introduction

Sodium nitrite is one of the well known ferroelectrics and extensive studies have been reported on the crystal structure at various temperatures (Ziegler, 1931; Strijk & MacGillavry, 1943; Kay & Frazer, 1961; Kay, 1972; Kay, Gonzalo & Maglic, 1975). In the present study the charge distribution in the NO_2^-

ion has been examined, which may be indispensable in estimating the lattice energy of the structure. In the calculation of the deformation density for the non-centrosymmetric structure, the spherical independent atom model (IAM) imposes a significant bias on the phase angle of the structure factor. This inadequacy should be removed by the aspherical-atom model (Hirshfeld, 1971; Harel & Hirshfeld, 1975; Ito & Shibuya, 1977). The present study adopted the multipole expansion method, and examined the negligibility of high-order multipoles. The necessity of this examination was discussed by Hansen (1988). To compare with the centrosymmetric case, the same investigation was made for $\text{LiNO}_2 \cdot \text{H}_2\text{O}$, for which X-ray intensity data collected at 120 K were available (Ohba, Kikkawa & Saito, 1985). The determination of the theoretical deformation density by an *ab initio* molecular-orbital calculation has been reported previously (Kikkawa, Ohba, Saito, Kamata & Iwata, 1987).

Experimental

Colorless prismatic crystals of NaNO_2 were grown from aqueous solution. A part of the hard crystal was ground by an Enraf–Nonius spherizer in a dry

* To whom correspondence should be addressed.